Synthesis of 2-Hydroxy-3-isopropoxypropyl Guar Gum and Its Thermo-responsive Property for Controlled Release

Ye Tian,[a,b,*] Yue Shang,[a,b] He Ma,[a,b] and Ying Liu [a,b,*]

2-Hydroxy-3-isopropoxypropyl guar gum (HIPGG), which is a novel polysaccharide-based thermo-responsive polymer, was synthesized *via* grafting a hydrophobic reagent (isopropyl glycidyl ether (IPGE)) onto a hydrophilic main backbone (guar gum (GG)). The HIPGG exhibited reversible and tunable thermo-responsive properties. Changing the molar substitution (MS) of the hydrophobic side chain enabled the lower critical solution temperature (LCST) to be adjusted within the range of 29.6 °C to 43.7 °C. Fluorescence spectrometry, dynamic light scattering (DLS), and transmission electron microscopy (TEM) were used to investigate the self-assembly behavior of HIPGG and the thermo-dependent size of its aggregates. It was demonstrated that HIPGG formed stable aggregates in aqueous solution, and the diameters of the aggregates increased as temperature increased. Subsequently, Nile red was used as a model to investigate the encapsulation and temperature-controlled release behaviors in HIPGG aggregates. The results indicated that Nile red was easily encapsulated in the hydrophobic region of HIPGG aggregates, and its release at 36 °C, 38 °C, and 42 °C revealed that temperature had a remarkable impact on release behavior.

Keywords: Thermo-responsive; Guar gum; Aggregates; Temperature-controlled release

Contact information: a: College of Marine Technology and Environment, Dalian Ocean University, Dalian 116023, China; b: Key Laboratory of Environment Controlled Aquaculture, Ministry of Education, Dalian Ocean University, Dalian, 116023, China;
**Corresponding authors: tianye@dlou.edu.cn; yingliu@dlou.edu.cn*

INTRODUCTION

Stimuli-responsive polymeric materials are a new class of materials that can change their physicochemical properties in response to external environmental factors, such as temperature, pH, ionic strength, and light intensity (Wu *et al.* 2016; Alejo *et al.* 2019; Yuba 2020). In recent years, stimuli-responsive polymers that have amphiphilic structures have received widespread attention in the field of biological medicine for two main reasons. First, these stimuli-responsive polymers self-assemble to form nanometer-sized aggregates or micelles that can be used as nanocarriers. Second, these micelles or aggregates can reversibly release or load encapsulated molecules under stimulation by external factors (Grzelczak *et al.* 2019).

Among these types of stimuli-responsive polymers, thermo-responsive polymers are the most intensively researched because their temperature changes are relatively easy to achieve and control. These polymers can also be conveniently and safely used in applications such as bio-separation, controlled release, and smart bioactive surfaces (Roy *et al.* 2013). Poly(N-isopropylacrylamide) (PINPAM) and its derivatives have been the most common thermo-responsive polymers. In aqueous solutions, PINPAM has a lower

critical solution temperature (LCST) that is close to the temperature of the human body. Thus, PINPAM has received widespread attention in the fields of biomedicine (Carter *et al.* 2006). PNIPAAM-based polymers can self-assemble into micelles that encapsulate drugs when the temperature is less than the LCST. In contrast, micelles are destabilized, and drugs are quickly released when the temperature is greater than the LCST. Obviously, the LCST is the most important parameter for thermo-responsive polymers, and accurate control of the LCST allows the thermo-responsive polymers to be used in different fields. Tuning the LCST of PNIPAAM-based polymers is generally performed *via* the addition of inorganic salts and solvents or copolymerization with other hydrophobic or hydrophilic monomers (Chen and Guan 2004; Nagase *et al.* 2018; Bordat *et al.* 2019).

In the past few decades, polysaccharide-based thermo-responsive polymers have been extensively researched because polysaccharides are naturally nontoxic, biocompatible, and biodegradable (Shen and Patel 2008). Typically, polysaccharide-based thermo-responsive materials can be prepared *via* the graft copolymerization of polysaccharides with synthetic thermo-responsive polymers (grafting-to) or monomers (grafting-from) (Graham *et al.* 2019). Guar gum (GG) is a biodegradable and biocompatible gum that is extracted from guar beans, and its main component is galactomannan, which is hydrophilic. In addition, the guar structure contains many highly reactive hydroxyl groups, which allow other chemical modifications to occur (Prabaharan 2011; Gupta *et al.* 2015; Wang *et al.* 2018). Due to these advantages, GG seems to be an ideal candidate for preparing thermo-responsive materials. Therefore, the grafting-to approach has been used to graft thermo-responsive polymers onto GG. GG-based thermo-responsive copolymers can be prepared *via* the grafting of semitelechelic PNIPAM or poly(ethyleneoxide-co-propylene oxide) onto a backbone of GG derivatives, and the LCST of copolymers is in accordance with that of synthetic thermo-responsive polymers (Gupta *et al.* 2011, 2015). In other words, the synthetic thermo-responsive polymer moieties control the LCST of these copolymers. Further, both copolymers can form micelles or aggregates in aqueous solution. However, these thermo-responsive copolymers have their own limitations (Atanase *et al.* 2017; Graham *et al.* 2019). First, it is difficult to tune their LCST because the methods for changing the thermo-responsive nature of a synthetic polymer are complex, and this limits their practical applications in different fields. Second, the use PNIPAM and other synthetic polymers in biomedical applications is problematic, as their monomers are toxic to humans, and they are not biodegradable. Because of these factors, it is of great interest to modify polysaccharides with nontoxic small molecules and achieve thermo-responsive behavior *via* controlling the balance between the hydrophilic and hydrophobic groups in polysaccharide-based polymers. In previous studies, a series of novel thermo-responsive cellulose-based polymers were synthesized *via* the grafting of hydrophobic short alkyl chains onto cellulose, and their LCSTs ranged from 17.1 °C to 56.1 °C. These amphiphilic polymers can also form micelles or aggregates when their concentration is above the critical aggregation concentration (CAC) (Tian *et al.* 2016; Dai *et al.* 2019a, 2019b).

In this study, a novel polysaccharide-based thermo-responsive polymer, namely 2-hydroxy-3-isopropoxypropyl guar gum (HIPGG) is reported. It was produced *via* the grafting of isopropyl glycidyl ether (IPGE) onto GG using an etherification reaction. Indeed, HIPGG exhibited reversible thermo-responsive behavior, and changing the molar substitution (MS) of the hydrophobic side chain and the salt concentrations could be used to tune LCST values. Further, HIPGG had an amphiphilic structure and could self-assemble into aggregates in aqueous solution, and the thermo-responsive behavior of the

HIPGG aggregates was investigated. Nile red was used as a model hydrophobic guest molecule, and the encapsulation and release behaviors of Nile red were investigated under different temperatures.

EXPERIMENTAL

Materials

The GG was purchased from Sigma-Aldrich (Saint Louis, MO, USA). Isopropyl glycidyl ether (IPGE) (> 96%) was purchased from Tokyo Chemical Industry Co., Ltd. (Tokyo, Japan). Pyrene and 9-diethylamino-5H-benzo[a]phenoxa-]phenoxazine-5-one (Nile red) were supplied by J&K Chemical, Ltd. (Beijing, China). Sodium chloride (NaCl, analytical reagent) and sodium hydroxide (NaOH, analytical reagent) were purchased from Damao Chemical Reagent Factory (Tian Jing, China). Sodium chloride, sodium carbonate, and sodium thiocyanate were purchased from Aladdin Industrial Corporation (Shanghai, China). All the chemical reagents were used as received without further treatment.

Preparation of 2-Hydroxy-3-isopropoxypropyl Guar Gum

The GG (1.0 g), deionized water (10 mL), and sodium hydroxide solution (1.6 g, 40%) were added to a 100-mL three-necked flask. The mixture was stirred and heated to 70 °C, and alkalization then proceeded for 1 h. IPGE (2.1 g, 2.5 g, 2.9 g, 3.3 g, 3.7 g) was then slowly added dropwise, and the temperature was increased to 80 °C. The reaction proceeded for 6 h. After reaction, the system was cooled to room temperature, and 1 M acetic acid was used to neutralize the solution to a pH of 7. The mixed solution was dialyzed for 72 h in a dialysis bag with a molecular weight cutoff of 8000 Da to 14000 Da. Most of the water in the resulting solution was removed using a rotary evaporator, and the remaining water was removed using a freeze-dryer (Biocool FD-1-135, Boyikang Experimental Instrument Co. LTD, Beijing, China) to obtain dried HIPGG.

Methods

The ^{1}H-NMR (^{1}H-nuclear magnetic resonance) spectra of HIPGG samples in D_2O were recorded on a Varian INOVA 500 spectrometer (Palo Alto, CA, USA). Transmittance at λ = 590 nm was monitored using a Mettler Toledo T90 (Zurich, Switzerland) with a temperature controller (LAUDA RP200) and a heating rate of 1 °C/min to determine the LCST values of the HIPGG solution. The LCST values were determined as the temperature at which the transmittance of the samples was around 50% relative to its original value.

Transmission electron microscopy (TEM, FEI TF30; FEI Company, Hillsboro, OR, USA) with an accelerating voltage of 80 kV was used to obtain images for analyzing the morphologies of HIPGG aggregates. The samples of HIPGG aggregates at temperatures below or above the LCST were prepared using a procedure similar to previously reported procedures (Tian *et al.* 2016). The dynamic light scattering (DLS) experiments were performed using a MalvernNano-ZS90 (Malvern Instruments, Malvern, England) with a He–Ne laser operated at 632 nm. The concentration of the samples was 1 g/L, and the samples were filtered using a filter with a pore diameter of 450 nm before measurement. The DLS measurements of the sample solutions were taken at temperatures in the range of 20 °C to 50 °C with a heating rate of 2 °C/min.

Determination of the CAC of HIPGG

A fluorescence spectrometer (Hitachi F7000; Hitachi Ltd., Tokyo, Japan) was used to measure the CAC of HIPGG. To use pyrene as a fluorescence probe, a syringe pump was used to add 10 μL of pyrene in acetone to a 10-mL volumetric flask. The solution was heated at 50 ^{o}C for 2 h to dry the acetone. Then, the HIPGG solution was added, and the flask was sonicated to dissolve the sample. The solution was then allowed to stand overnight. The measurement conditions were as follows: an emission wavelength of 373 nm, a scanning range of 305 nm to 365 nm, and a measurement temperature of 20 °C.

Encapsulation and Release of Nile Red

A fluorescence spectrometer (Hitachi F7000) with an excitation wavelength of 490 nm was used to determine the behaviors of encapsulation and temperature-controlled release of Nile red. The preparation of each aqueous solution of HIPGG with a constant concentration of Nile red was carried out according to the procedure described in previous literature (Kim *et al.* 2009; Park *et al.* 2010; Tian *et al.* 2016). Nile red in a solution of acetone was added to a 10-mL volumetric flask, and the acetone was removed *via* evaporation. Aqueous solutions with different concentrations of HIPGG were each loaded into a volumetric flask and sonicated in an ice bath for 4 h. Then, the solutions stood overnight. The final Nile red concentration in each aqueous solution of HIPGG samples was 20 mg/L. All samples were filtered using a 450-nm filter before measurement. In the temperature-controlled release experiment of Nile red, the samples were maintained at 36 °C, 38 °C, or 42 °C. Then, the samples were used to investigate the release behaviors under these temperatures, and each sample was monitored for three independent measuring results from which average values were obtained.

RESULTS AND DISCUSSION

Synthesis and Characterization of HIPGG

The synthetic route for HIPGG is shown in Fig. 1. The main chain GG is hydrophilic and reacted with the hydrophobic reagent (IPGE). Adjusting the amount of hydrophobic reagent enabled HIPGG with different MS to be obtained. Table 1 illustrates the characteristic parameters of HIPGG with different MS and the thermo-responsive properties of its aqueous solutions.

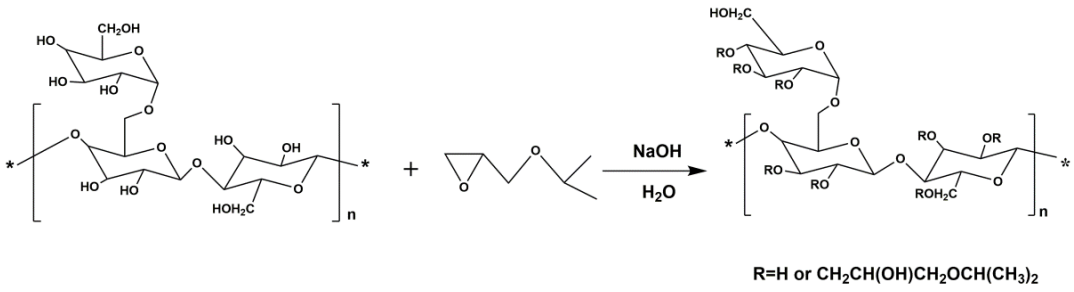

Fig. 1. Synthetic route for HIPGG

Figure 2 shows the ^{1}H-NMR spectra of HIPGG. The signals at 1.08 ppm were characteristic of the isopropyl group (H8). The signals at 5.30 ppm to 5.80 ppm were ascribed to the anomeric protons (H1) of HIPGG-3, and these indicated partial substitution

at the hydroxyl of the O-2 position. The broader signal between 3.30 ppm and 4.40 ppm corresponded to protons of the anhydroglucose units and protons of the O–CH_2–CHOH–CH_2–O–CH_2 group. The MS of HIPGG was expressed using the ratio of the integrated peak area of the methyl in the isopropyl group to six times the integrated peak area of H1 in the anhydroglucose unit (AGU). These results indicated successful etherification.

Table 1. Preparation and Characterization of HIPGG

Sample	n(IPGE):n(AGU) [a]	MS [b]	LCST (°C) [c]	CAC at 20 °C (g/L) [d]
HIPGG-1	3.0	0.98 ± 0.02	43.7 ± 1.7	0.108 ± 0.012
HIPGG-2	3.5	1.19 ± 0.03	41.2 ± 1.2	0.071 ± 0.008
HIPGG-3	4.0	1.42 ± 0.04	37.1 ± 1.0	0.051 ± 0.006
HIPGG-4	4.5	1.63 ± 0.01	34.1 ± 1.4	0.046 ± 0.009
HIPGG-5	5.0	2.01 ± 0.05	29.6 ± 1.1	0.031 ± 0.005

[a]Mole ratio of etherifying agent to glucose units of guar gum
[b]MS was determined by ^{1}H-NMR
[c]Determined *via* a Mettler Toledo T90 with a LAUDA RP200 temperature controller
[d]CAC was determined via a Hitachi F7000 fluorescence spectrometer
IPGE: Isopropyl glycidyl ether; AGU: Anhydroglucose units; MS: Molar substitution; LCST: Lower critical solution temperature; HIPGG: 2-Hydroxy-3-isopropoxypropyl guar gum
Values of MS, LCST, and CAC are mean of three experiments ± SD.

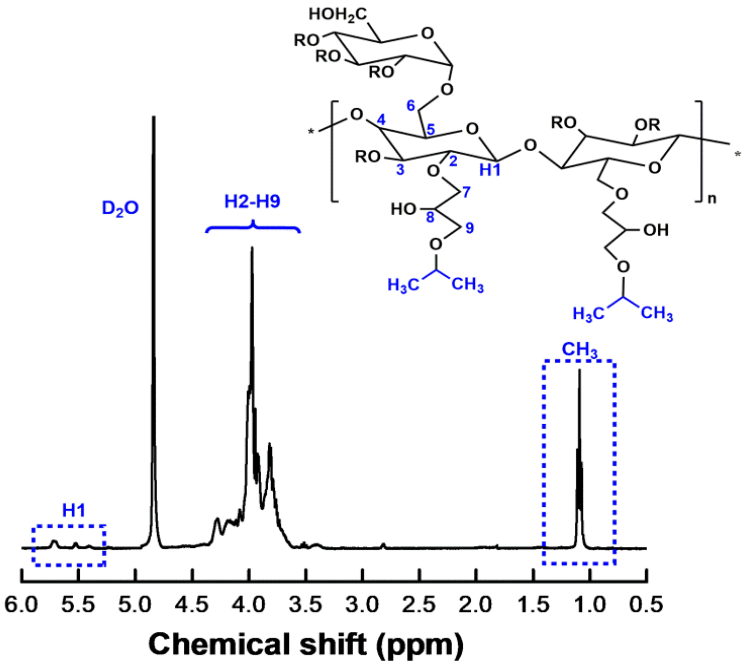

Fig. 2. The ^{1}H-NMR spectra of HIPGG-3 recorded in D_2O

Thermo-responsive Behavior of HIPGG Solutions

The LCST is among the most important parameters for describing thermo-responsive properties of polymers. Figure 3a shows that the samples of aqueous solutions of HIPGG were transparent below their LCST, and the solution became turbid when the temperature increased above the LCST. When the temperature was decreased, the solution became transparent again. This indicated that the thermo-responsive phase-separation behavior of the HIPGG aqueous solution was reversible in nature.

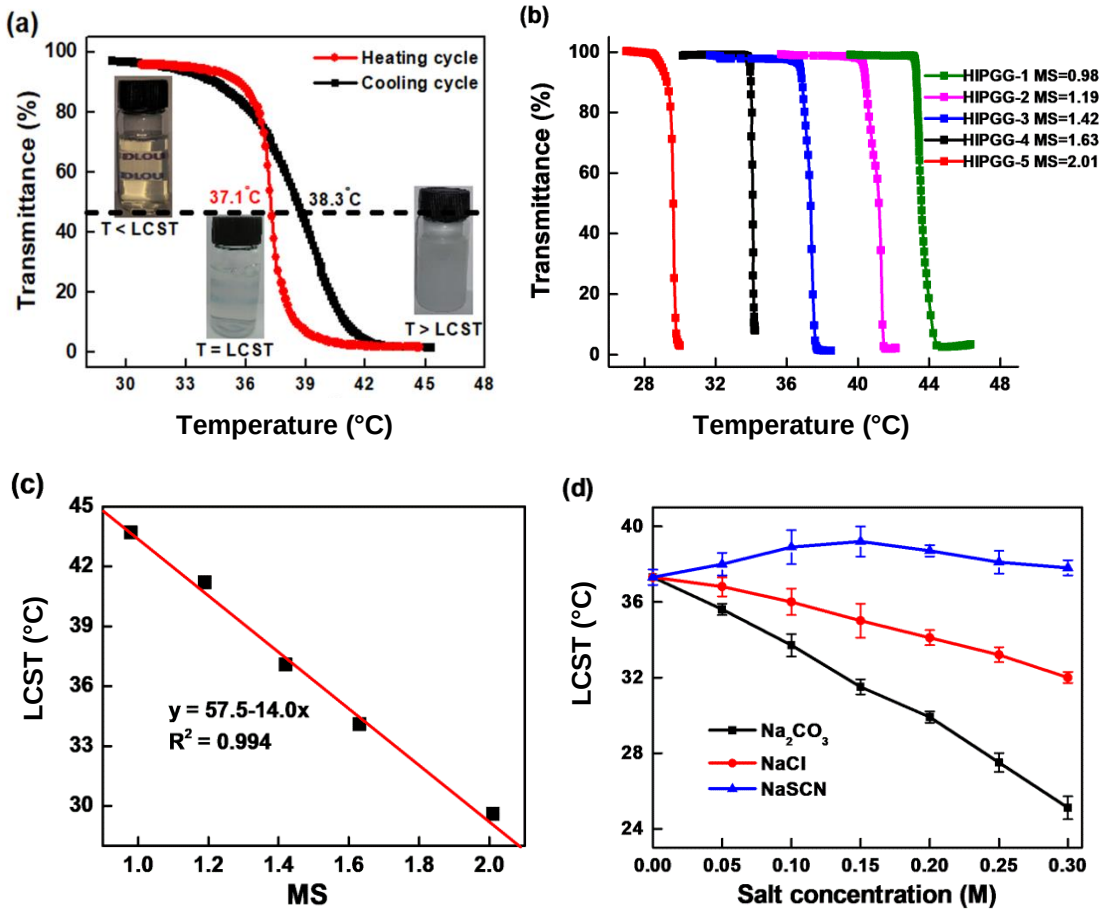

Fig. 3. (a) Plots of transmittance as a function of temperature measured for aqueous solutions (1 g/L) of HIPGG-3 (insets show visual changes of the transmittance of sample solutions below and above the LCST); (b) Transmittance changes for aqueous solutions (1 g/L) of HIPGG-1 to HIPGG-5; (c) Plot of the measured LCSTs as a function of MS; (d) Plots of the measured LCSTs as a function of Na_2CO_3, NaCl, and NaSCN concentrations

The aqueous solution of HIPGG-3 (1 g/L) exhibited hysteresis of 1.2 °C in the LCST during the cooling process (38.3 °C) relative to the heating process (37.1 °C) (Fig. 3a). Figure 3b shows the changes in transmittance for aqueous solutions of HIPGG with different MS (1 g/L) *vs.* temperature. The transmittance of all the HIPGG solutions with different MS decreased sharply when the temperature was increased to the LCSTs. For example, the transparent HIPGG-3 aqueous solution became turbid when the temperature was increased to 37.1 °C (Fig. 1a). This was because the hydrophilic framework (GG) of HIPGG formed hydrogen bonds with water molecules at low temperatures. Thus, HIPGG could dissolve in water. Conversely, when the temperature was increased to the LCST, the hydrogen bonds between HIPGG and water molecules were destroyed. Subsequently, the interactions between hydrophobic alkyl chains become dominant, which caused aggregation of the HIPGG molecules, and the LCST exhibited linear decreases with increases in the MS. Specifically, as seen in Fig. 3c, the LCST decreased from 43.7 °C to 29.6 °C when the MS was increased from 0.98 to 2.01. This showed that varying the MS of isopropyl glycidyl ether enabled the LCST of HIPGG to be precisely adjusted. As temperature increased, the HIPGGs with higher MS possessed stronger hydrophobic association between molecules, which led to decreases in LCST. Notably, the HIPGG

samples that had MS values in the range of 0.98 to 2.01 had a desirable thermo-responsive property. However, when the MS was less than 0.98, the HIPGG solution did not have phase separation behavior during heating, which was because of the low number of hydrophobic side chains and the weak hydrophobicity. When the MS was greater than 2.01, HIPGG did not dissolve in water because of its excessively strong hydrophobicity.

Adding inorganic salts could also be used to adjust the LCST of HIPGG aqueous solution. Plots exhibiting the variations in transmittance with respect to the temperature at different concentrations of NaSCN, NaCl, or Na_2CO_3 are given in Fig. 3d for an HIPGG-3 concentration of 1 g/L. When the concentrations of NaCl and Na_2CO_3 were increased from 0 M to 0.3 M, the LCST of HIPGG decreased linearly from 37.1 °C to 34.4 °C and 27.3 °C, respectively. As mentioned above, HIPGG could be dissolved in water because of hydrogen bonding between HIPGG and water. When NaCl or Na_2CO_3 was added to the solution, the hydrogen bonding between HIPGG and water molecules weakened. This resulted in easier removal of water molecules from the HIPGG molecular chain during heating, which reduced the LCST. In contrast, in the presence of NaSCN, the variations of LCST were nonlinear with respect to concentration. Specifically, the LCST increased as the NaSCN concentration increased, which was followed by a decrease at larger concentrations of NaSCN. The added SCN^- complexed with the hydroxyl groups on the HIPGG molecular chain, which increased the solubility of HIPGG, thereby increasing the LCST. The presence of these three kinds of inorganic salts affected the LCSTs in accordance with the Hofmeister series (Yan and Mu 2015; Yan *et al.* 2016).

Self-aggregation of HIPGG in Aqueous Solution

Similar to PINPAM, amphiphilic HIPGG self-assembles into aggregates when it is at a certain concentration in water. In this study, fluorescence spectrometry with pyrene as a fluorescence probe was used to study the formation of HIPGG aggregates. The solubility of pyrene in aqueous solutions is small. However, in a hydrophobic environment, the fluorescence spectrum of pyrene changes considerably, and thus pyrene is often used to determine the CAC. Figure 4a shows the excitation spectrum of pyrene with HIPGG-3 at different concentrations. With the increase in the HIPGG-3 concentration from 0.0005 g/L to 0.7 g/L, the intensity of the fluorescence excitation spectra of pyrene gradually increased. The maximum peak intensity of the excitation spectrum of pyrene red-shifted from 334 nm to 338 nm when the aqueous solution of HIPGG-3 reached a certain concentration. This indicated that the polarity of the environment of pyrene changed from a polar environment to a weakly polar or nonpolar environment. This also indicated that HIPGG aggregates formed and encapsulated pyrene in the hydrophobic region of the aggregates. The intensity ratio of the peaks at 338 nm and 334 nm (I_{338}/I_{334}) was calculated and plotted *versus* the HIPGG-3 concentrations (Fig. 4b). The sharp increase in the intensity ratio of the pyrene peaks at 338 nm and 334 nm in the excitation spectra indicated that the CAC for HIPGG-3 was approximately 0.051 g/L. In addition, the CAC values of the HIPGG samples decreased as MS increased (Fig. 4c). The HIPGG samples that had higher MS possessed stronger hydrophobicity, which caused hydrophobic interactions among HIPGG molecules to occur more easily; thus, the CAC decreased.

Dynamic light scattering and TEM were used to investigate variations in the size of the HIPGG-1 to HIPGG-5 aggregates with respect to temperature. As can be seen in Fig. 4d, in the lower temperature ranges, the diameters of the HIPGG-1 to HIPGG-5 aggregates were relatively small, and there were no noticeable changes.

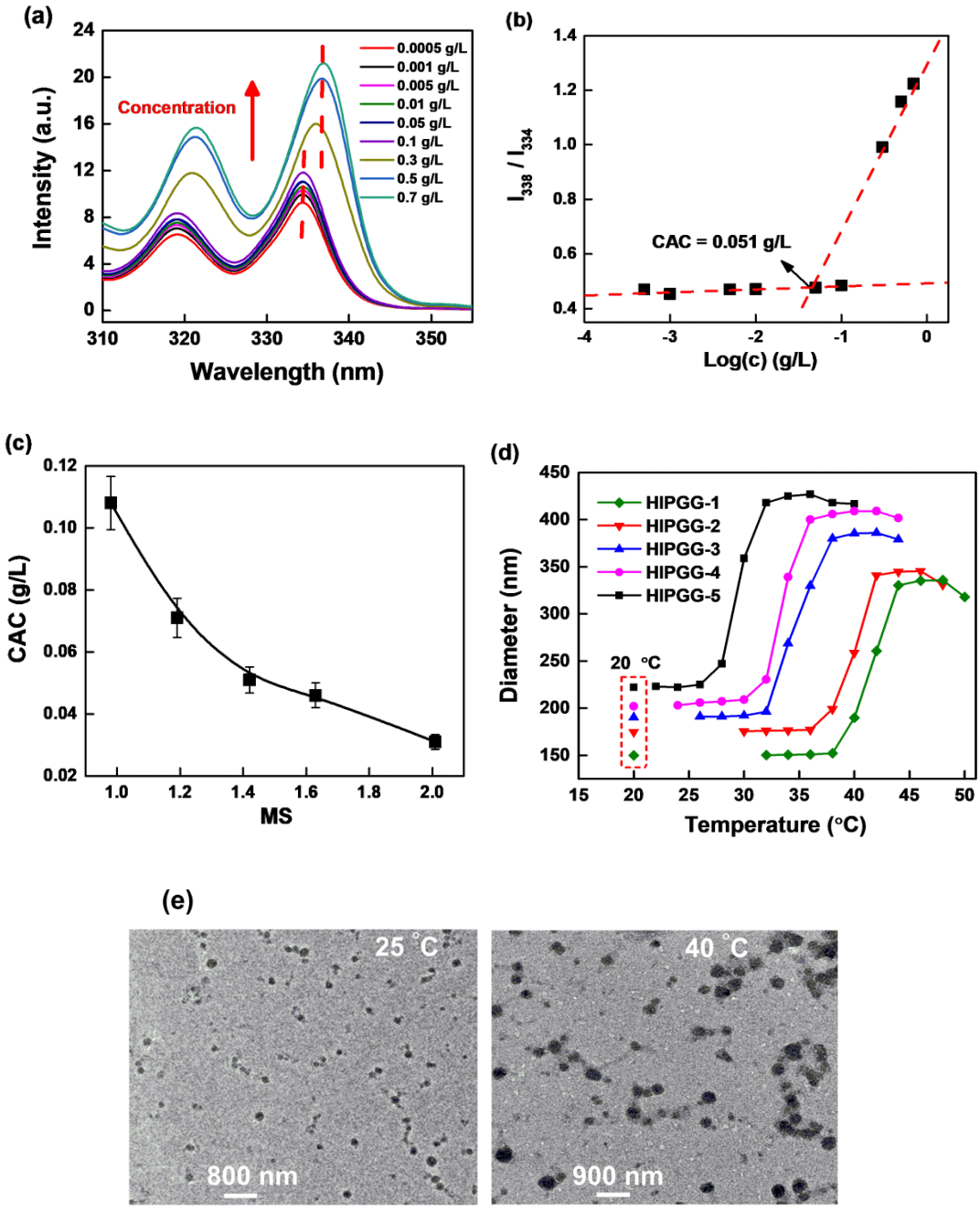

Fig. 4. (a) Excitation spectra of pyrene; (b) I_{338}/I_{334} values of aqueous solutions of HIPGG-3 at different concentrations (pyrene concentration of 6×10^{-7} M and λ_{em} = 490 nm); (c) Plots of the measured CAC as a function of MS; (d) Temperature dependence of hydrodynamic diameters for HIPGG-1 to HIPGG-5 aggregates in aqueous solutions (concentration of 1 g/L); (e) TEM images of HIPGG-3 aggregates at 25 °C and 40 °C

For example, the diameter of HIPGG-3 aggregates was approximately 191 nm in the range of 20 °C to 32 °C. The values of the hydrodynamic diameter of the HIPGG-1 to HIPGG-4 aggregates were smaller than that of HIPGG-5. This was because the HIPGG samples with higher MS were more hydrophobic and thus formed a larger hydrophobic region, which resulted in an increase in the diameters of the aggregates. In contrast, the

size of the HIPGG-1 to HIPGG-5 aggregates increased rapidly in the higher temperature ranges. For example, when the temperature was increased from 32 °C to 38 °C, the size of the HIPGG-3 aggregates increased sharply from 191 nm to 385 nm. Remarkably, the size of the aggregates decreased slightly when the temperature of the solution was increased from 42 °C to 44 °C, which was probably because the solutions of the aggregates further heated up as a result of dehydration and shrinkage. This result was similar to that observed for aggregates of poly(2-alkyl-2-oxazoline)s (Obeid *et al.* 2009).

To provide further support for the DLS results, TEM was performed to monitor changes in the morphology and size of the HIPGG aggregates upon increasing the temperature increase from 25 °C to 40 °C. Figure 4e shows that smaller aggregates of HIPGG-3 (average diameter of approximately 176 nm) were observed at 25 °C, whereas larger aggregates (average diameter of approximately 368 nm) were observed at 40 °C. Remarkably, the size of the aggregates that were observed *via* TEM at temperatures in the range of 25 °C and 40 °C was smaller than that determined *via* DLS. This may have been because dehydration of the aggregates was induced by water evaporation, which resulted in the shrinkage of aggregates in the TEM experiment (Yuan *et al.* 2011; Ten Brummelhuis *et al.* 2012).

Encapsulation of Nile Red and Its Temperature-controlled Release

Fluorescence spectroscopy with Nile red as a model for a hypothetical drug was used to study the encapsulation and temperature-controlled release behaviors of the HIPGG aggregates. Nile red is mostly insoluble in water, it presents little fluorescence signal. However, the fluorescence intensity of Nile red dramatically increases when it is in a hydrophobic environment, such as when it is in the hydrophobic region of aggregates (Chen and Guan 2004). In this study, the fluorescence intensity of Nile red was investigated using photoluminescence spectroscopy with an excitation wavelength of 490 nm with HIPGG-3 at different concentrations. Figure 5a shows that the fluorescence intensity of Nile red was invisible in the absence of HIPGG-3 aggregates. However, there was a clear intense peak at 625 nm observed when HIPGG-3 was in aqueous solution. In addition, the fluorescence intensity of Nile red was relatively weak when the concentration of the HIPGG-3 solution was lower than its CAC, whereas it increased rapidly when the concentration was above its CAC. Many HIPGG-3 aggregates formed above the CAC, which provided a larger hydrophobic region for encapsulating Nile red and contributed to the increased intensity (Kim *et al.* 2009; Park *et al.* 2010). A similar tendency was also observed for other HIPGG samples that had different MS (Fig. 5b). Specifically, the fluorescence intensities at maximum values were plotted against the concentration of HIPGG-1 to HIPGG-5. For all the HIPGG samples, the fluorescence intensity at λ_{max} for Nile red exhibited a steady increase with respect to the concentration of samples, and there was a relatively rapid increase observed when the concentration was above the CAC.

The encapsulation of Nile red in HIPGG aggregates could be controllably released in response to various temperatures. The release of Nile red from HIPGG aggregates was examined using fluorescence spectrometry because the fluorescence intensity of Nile red decreased dramatically in aqueous solution compared to that in the hydrophobic region of the HIPGG aggregates. Thus, the fluorescence intensity of Nile red that was encapsulated in HIPGG aggregates was measured over time at 36 °C, 38 °C, and 42 °C. Figure 5c shows that the temperature control of the release behavior of the aggregates.

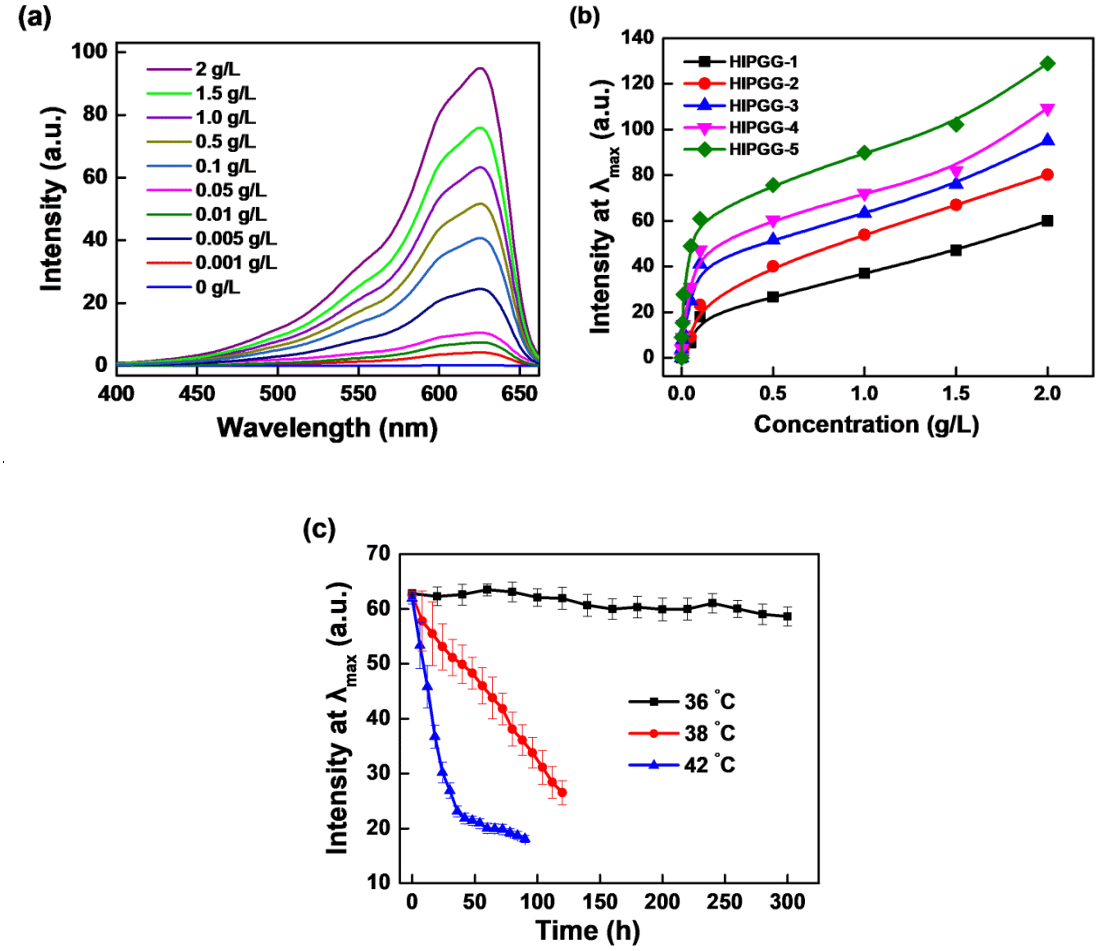

Fig. 5. (a) Emission spectra for Nile red in aqueous solutions with different concentrations of HIPGG-3 (λ_{ex}= 490 nm); (b) Fluorescence intensity at λ_{max} for the emission spectra of Nile red as a function of concentration of HIPGG-1 to HIPGG-5; (c) Nile red fluorescence in the aggregates of HIPGG-3 as a function of time at 36 °C, 38 °C, and 42 °C

The fluorescence intensity of Nile red in HIPGG-3 aggregates did not obviously decrease during incubation for 300 h at 36 °C, it was indicated that Nile red could be stably present in HIPGG aggregates when the temperature was lower than LCST. However, the intensity of Nile red gradually decreased during incubation for 120 h at 38 °C (LCST = 37.1 °C). When the temperature was higher than the LCST of HIPGG, the hydrophilic shell collapsed. This resulted in deformation of the aggregate structure, and the Nile red was released from the hydrophobic region to the aqueous solution, which led to the fluorescence quenching of Nile red. In addition, changing the temperatures enabled the encapsulated guest molecules to be easily and controllably released from HIPGG aggregates (Fig. 5c), and the fluorescence intensity decreased more rapidly at higher temperatures. Interestingly, at 42 °C, the fluorescence intensity remained constant after 50 h, and no further obvious decrease in the fluorescence intensity of Nile red was monitored. This was in line with the results of other amphiphilic thermo-responsive polymers (Bose *et al.* 2017). Nile red remained encapsulated in the collapsed HIPGG-3 aggregates because of shrinkage at 42 °C to 44 °C.

CONCLUSIONS

1. In this work, a novel guar gum-based thermo-responsive polymer (HIPGG) was synthesized *via* etherification reaction, and it had a tunable lower critical solution temperature (LCST). Changing the molar substitution (MS) of the hydrophobic chain enabled the LCST of HIPGG to be tuned. Specifically, when the MS of HIPGG increased from 0.98 to 2.01, the LCST decreased from 43.7 °C to 29.6 °C. In addition, inorganic salts (NaSCN, NaCl, and Na_2CO_3) had a remarkable effect on the LCST of HIPGG.
2. Fluorescence spectroscopy, DLS, and TEM were used to research the self-assembly behavior and thermo-responsive property of HIPGG aggregates. Investigations showed that temperature changes could be used to change the size and structure of the HIPGG aggregates.
3. The behaviors of encapsulation and release of Nile red in HIPGG aggregates were investigated at temperatures above and below the LCST. At temperatures below the LCST of HIPGG, the Nile red was stably encapsulated in HIPGG aggregates, whereas it was released from aggregates when the temperature was higher than the LCST. Additionally, changing the temperature of the aqueous solution of HIPGG-Nile red enabled control of the release rate of Nile red. In brief, HIPGG aggregates with desirable thermo-responsive properties have broad application prospects in drug release platforms and in other appropriate biological research.

ACKNOWLEDGMENTS

The authors are grateful for the support of the National Key R&D Program of China (No. 2017YFD0701700), the National Natural Science Foundation of China (No. 31901775 and No. 31672673), the Key R&D Program of Guangdong Province (No. 2019B020215001), and the Liaoning S&T Project (No. 2017203002).

REFERENCES CITED

Alejo, T., Uson, L., and Arruebo, M. (2019). "Reversible stimuli-responsive nanomaterials with on-off switching ability for biomedical applications," *Journal of Controlled Release* 314, 162-176. DOI: 10.1016/j.jconrel.2019.10.036

Atanase, L. I., Desbrieres, J., and Riess, G. (2017). "Micellization of synthetic and polysaccharides-based graft copolymers in aqueous media," *Progress in Polymer Science* 73, 32-60. DOI: 10.1016/j.progpolymsci.2017.06.001

Bordat, A., Boissenot, T., Nicolas, J., and Tsapis, N. (2019). "Thermoresponsive polymer nanocarriers for biomedical applications," *Advanced Drug Delivery Reviews* 138, 167-192. DOI: 10.1016/j.addr.2018.10.005

Bose, A., Jana, S., Saha, A., and Mandal, T. K. (2017). "Amphiphilic polypeptide-polyoxazoline graft copolymer conjugate with tunable thermoresponsiveness: Synthesis and self-assembly into various micellar structures in aqueous and nonaqueous media," *Polymer* 110, 12-24. DOI: 10.1016/j.polymer.2016.12.068

Carter, S., Rimmer, S., Rutkaite, R., Swanson, L., Fairclough, J. P. A., Sturdy, A., and Webb, M. (2006). "Highly branched poly(*N*-isopropylacrylamide) for use in protein purification," *Biomacromolecules* 7(4), 1124-1130. DOI: 10.1021/bm050929h

Chen, G. H., and Guan, Z. B. (2004). "Transition metal-catalyzed one-pot synthesis of water-soluble dendritic molecular nanocarriers," *Journal of the American Chemical Society* 126(9), 2662-2663. DOI: 10.1021/ja039829e

Dai, M., Liu, Y., Ju, B., and Tian, Y. (2019a). "Preparation of thermoresponsive alginate/starch ether composite hydrogel and its application to the removal of Cu(II) from aqueous solution," *Bioresource Technology* 294, Article ID 122192. DOI: 10.1016/j.biortech.2019.122192

Dai, M., Tian, Y., Fan, J., Ren, J., Liu, Y., Rahman, M., Ju, B., Ren, X., and Ma, H. (2019b). "Tuning of lower critical solution temperature of thermoresponsive 2-hydroxy-3-alkoxypropyl hydroxyethyl cellulose by alkyl side chains and additives," *BioResources* 14(4), 7977-7991. DOI: 10.15376/biores.14.4.7977-7991

Graham, S., Marina, P. F., and Blencowe, A. (2019). "Thermoresponsive polysaccharides and their thermoreversible physical hydrogel networks," *Carbohydrate Polymers* 207, 143-159. DOI: 10.1016/j.carbpol.2018.11.053

Grzelczak, M., Liz-Marzán, L. M., and Klajn, R. (2019). "Stimuli-responsive self-assembly of nanoparticles," *Chemical Society Reviews* 48(5), 1342-1361. DOI: 10.1039/c8cs00787j

Gupta, N. R., Ghute, P. P., and Badiger, M. V. (2011). "Synthesis and characterization of thermo-sensitive graft copolymer of carboxymethyl guar and poly(*N*-isopropylacrylamide)," *Carbohydrate Polymers* 83(1), 74-80. DOI: 10.1016/j.carbpol.2010.07.023

Gupta, N. R., Torris, A. A. T., Wadgaonkar, P. P., Rajamohanan, P. R., Ducouret, G., Hourdet, D., Creton, C., and Badiger, M. V. (2015). "Synthesis and characterization of PEPO grafted carboxymethyl guar and carboxymethyl tamarind as new thermo-associating polymers," *Carbohydrate Polymers* 117, 331-338. DOI: 10.1016/j.carbpol.2014.09.073

Kim, S. H., Tan, J. P. K., Nederberg, F., Fukushima, K., Yang, Y. Y., Waymouth, R. M., and Hedrick, J. L. (2009). "Mixed micelle formation through stereocomplexation between enantiomeric poly(lactide) block copolymers," *Macromolecules* 42(1), 25-29. DOI: 10.1021/ma801739x

Nagase, K., Yamato, M., Kanazawa, H., and Okano, T. (2018). "Poly(*N*-isopropyl-acrylamide)-based thermoresponsive surfaces provide new types of biomedical applications," *Biomaterials* 153, 27-48. DOI: 10.1016/j.biomaterials.2017.10.026

Obeid, R., Maltseva, E., Thünemann, A. F., Tanaka, F., and Winnik, F. M. (2009). "Temperature response of self-assembled micelles of telechelic hydrophobically modified poly(2-alkyl-2-oxazoline)s in water," *Macromolecules* 42(6), 2204-2214. DOI: 10.1021/ma802592f

Park, J., Moon, M., Seo, M., Choi, H., and Kim, S. Y. (2010). "Well-defined star-shaped rod-coil diblock copolymers as a new class of unimolecular micelles: Encapsulation of guests and thermoresponsive phase transition," *Macromolecules* 43(19), 8304-8313. DOI: 10.1021/ma101567p

Prabaharan, M. (2011). "Prospective of guar gum and its derivatives as controlled drug delivery systems," *International Journal of Biological Macromolecules* 49(2), 117-124. DOI: 10.1016/j.ijbiomac.2011.04.022

Roy, D., Brooks, W. L. A., and Sumerlin, B. S. (2013). "New directions in thermoresponsive polymers," *Chemical Society Reviews* 42(17), 7214-7243. DOI: 10.1039/c3cs35499g

Shen, L., and Patel, M. K. (2008). "Life cycle assessment of polysaccharide materials: A review," *Journal of Polymers and the Environment* 16, 154-167. DOI: 10.1007/s10924-008-0092-9

Ten Brummelhuis, N., Secker, C., and Schlaad, H. (2012). "Hofmeister salt effects on the LCST behavior of poly(2-oxazoline) star ionomers," *Macromolecular Rapid Communications* 33(19), 1690-1694. DOI: 10.1002/marc.201200406

Tian, Y., Ju, B., Zhang, S., and Hou, L. (2016). "Thermoresponsive cellulose ether and its flocculation behavior for organic dye removal," *Carbohydrate Polymers* 136, 1209-1217. DOI: 10.1016/j.carbpol.2015.10.031

Wang, C., Yang, T., Wang, T., and Qiu, L. (2018). "Thermosensitive behavior of hydrophobically associating anionic guar gum solutions and gels," *International Journal of Biological Macromolecules* 111, 169-177. DOI: 10.1016/j.ijbiomac.2018.01.017

Wu, W., Li, J., Liu, W., and Deng, Y. (2016). "Temperature-sensitive, fluorescent poly(N-isopropyl-acrylamide)-grafted cellulose nanocrystals for drug release," *Bioresources* 11(3), 7026-7035. DOI: 10.15376/biores.11.3.7026-7035

Yan, C., and Mu, T. (2015). "Molecular understanding of ion specificity at the peptide bond," *Physical Chemistry Chemical Physics* 17(5), 3241-3249. DOI: 10.1039/c4cp04055d

Yan, C., Xue, Z., Zhao, W., Wang, J., and Mu, T. (2016). "Surprising Hofmeister effects on the bending vibration of water," *ChemPhysChem* 17(20), 3309-3314. DOI: 10.1002/cphc.201600551

Yuan, W., Li, X., Gu, S., Cao, A., and Ren, J. (2011). "Amphiphilic chitosan graft copolymer *via* combination of ROP, ATRP and click chemistry: Synthesis, self-assembly, thermosensitivity, fluorescence, and controlled drug release," *Polymer* 52(3), 658-666. DOI: 10.1016/j.polymer.2010.12.052

Yuba, E. (2020). "Development of functional liposomes by modification of stimuli-responsive materials and their biomedical applications," *Journal of Materials Chemistry B* 8(6), 1093-1107. DOI: 10.1039/c9tb02470k

Article submitted: June 15, 2020; Peer review completed: August 8, 2020; Revised version received and accepted: August 14, 2020; Published: August 19, 2020.
DOI: 10.15376/biores.15.4.7615-7627